EUROPEAN ORGANIZATION FOR NUCLEAR RESEARCH
CERN - ACCELERATORS AND TECHNOLOGY SECTOR

CERN-ATS-2011-230

ELECTRICAL RESISTANCE OF Nb_3Sn/Cu SPLICES PRODUCED BY ELECTROMAGNETIC PULSE TECHNOLOGY AND SOFT SOLDERING

D. Schoerling, S. Heck, C. Scheuerlein, S. Atieh
CERN, Geneva, Switzerland
R. Schaefer
PSTproducts GmbH, Alzenau, Germany

Abstract

The electrical interconnection of Nb_3Sn/Cu strands is a key issue for the construction of Nb_3Sn based damping ring wigglers and insertion devices for third generation light sources. We compare the electrical resistance of Nb_3Sn/Cu splices manufactured by solid state welding using Electromagnetic Pulse Technology (EMPT) with that of splices produced by soft soldering with two different solders. The resistance of splices produced by soft soldering depends strongly on the resistivity of the solder alloy at the operating temperature. By solid state welding splice resistances below 10 nΩ can be achieved with 1 cm strand overlap length only, which is about 4 times lower than the resistance of Sn96Ag4 soldered splices with the same overlap length. The comparison of experimental results with Finite Element simulations shows that the electrical resistance of EMPT welded splices is determined by the resistance of the stabilizing copper between the superconducting filaments and confirms that welding of the strand matrix is indeed achieved. EMPT allows interconnecting the ductile, unreacted strands, which reduces the risk of damaging the brittle reacted Nb_3Sn strands.

To be published in Superconductor Science and Technology

Geneva, Switzerland

November 2011

Electrical resistance of Nb_3Sn/Cu splices produced by Electromagnetic Pulse Technology and soft soldering

D. Schoerling, S. Heck, C. Scheuerlein*, S. Atieh

European Organization for Nuclear Research (CERN), CH-1211 Geneva, Switzerland

R. Schaefer

PSTproducts GmbH, Alzenau, Germany

Abstract

The electrical interconnection of Nb_3Sn/Cu strands is a key issue for the construction of Nb_3Sn based damping ring wigglers and insertion devices for third generation light sources. We compare the electrical resistance of Nb_3Sn/Cu splices manufactured by solid state welding using Electromagnetic Pulse Technology (EMPT) with that of splices produced by soft soldering with two different solders. The resistance of splices produced by soft soldering depends strongly on the resistivity of the solder alloy at the operating temperature. By solid state welding splice resistances below 10 nΩ can be achieved with 1 cm strand overlap length only, which is about 4 times lower than the resistance of Sn96Ag4 soldered splices with the same overlap length. The comparison of experimental results with Finite Element simulations shows that the electrical resistance of EMPT welded splices is determined by the resistance of the stabilizing copper between the superconducting filaments and confirms that welding of the strand matrix is indeed achieved. EMPT allows interconnecting the ductile, unreacted strands, which reduces the risk of damaging the brittle reacted Nb_3Sn strands.

* electronic mail: Christian.Scheuerlein@cern.ch

1 Introduction

Nb_3Sn/Cu lap joints are a key issue for Nb_3Sn based insertion devices for third generation light sources. Interest rises in superconducting insertion devices because they may provide the means to generate hard x-ray light with high spectral brightness. Horizontal racetrack damping wiggler magnets, as they are developed for the Compact Linear Collider (CLIC) study [1], are another application that may require 15,000 Nb_3Sn/Cu electrical interconnections. The failure of one of them would prohibit the operation of the magnets. The splice specifications are set by the heat load from the electrical power dissipated in the resistive Nb_3Sn/Cu splices and the mechanical strength of the splices.

Soft soldering is commonly used for the electrical interconnection of superconducting strands. In order to study the influence of the solder resistivity on the overall splice resistance we have measured the resistance of splices produced with two solder alloys (Sn96Ag4 and Sn77.2In20Ag2.8) which exhibit strongly different electrical resistivity at cryogenic temperatures. The Sn96Ag4 solder alloy has comparable electrical resistivity as pure Sn, and it is the solder that has the lowest resistivity of typically used solders [2], while the 4.2 K the resistivity of the Sn77.2In20Ag2.8 solder alloy that was also used in this study is about 160 times higher [3].

Soft soldering before Nb_3Sn reaction is not possible since the solder would diffuse into the strand matrix during the reaction heat treatment at typically 700 °C. In order to minimize the risk of damaging the fragile A15 phase it can be advantageous to interconnect the ductile strands before reaction. Therefore, we are studying alternative methods that allow to interconnect the ductile pre-cursor.

Previously we have reported resistance results for superconducting wire splices produced by electrolytic Cu deposition [4]. Solid state welding is another possible way to interconnect superconducting strands. Ultrasonic (US) welding, as an example, is the state-of-the-art technology for the electrical interconnection of ductile Nb-Ti/Cu composite superconducting strands. About 35,000 splices with a strand over lap length of 1 cm with resistances below 10 nΩ have been routinely achieved during the construction of the Large Hadron Collider (LHC) [5].

Here we study splices produced by Electromagnetic Pulse Technology (EMPT) welding, another method that can connect Nb_3Sn/Cu wires before reaction. The splices have been characterized by resistance measurements in liquid Helium, optical metallography, peel tests and indentation hardness measurements. Electrical resistance results are compared and complemented with Finite Element (FE) simulations performed with COMSOL Multiphyisics.

2 Experimental

2.1 The superconductor samples

All splices were prepared using Oxford superconducting technology (OI-ST) high-J_c Restack-Rod-Process (RRP) Nb_3Sn/Cu strands (billet #7419) [6]. The strand with a

nominal diameter of 0.8 mm contains 54 Nb-Ta alloy filament bundles, each surrounded by distributed diffusion barriers, which thickness is roughly 0.5 µm, and locally less than 0.1 µm [4]. The strand has an effective filament diameter of about 80 µm, and it can reach non-Cu critical current density values close to 3000 A mm^{-2} at 12 T and 4.2 K.

2.2 Preparation of splice samples with electromagnetic pulse technology

The ElectroMagnetic Pulse Technology (EMPT) process is based on induction of a current pulse in an electrical conductive workpiece by a coil. The coil is loaded by a strong but short time current pulse of about 800 kA. Due to Lentz rule, the current induced into the workpiece opposes the coil current. Hence, a magnetic force acts on the work piece. In case of high magnetic flux generated by the EMPT coil, this force is strong enough to deform the work piece in the area loaded by magnetic force and to accelerate the deformed material up to velocities of several 100 m/s within some microseconds [7]. If the accelerated portion of the workpiece impacts another metallic contact partner, high contact stresses are generated. The result is a severe plastic deformation of the interfacial surface which cracks up the oxide layers, covering the workpiece surface. The generated metallic pure surfaces of both contact partners are highly reactive. The contact normal pressure exceeds the metals yield strength by a factor of 5-10. Hence, the interfaces of both contact partners are pressed so close together, that an electron exchange between the two metal lattices is accomplished and a metallic bond is established. As EMPT welding does not require the workpiece temperature to be elevated, it is classified as a solid state welding process. Figure 1 illustrates the bonding mechanism and the geometry of the bonding zone.

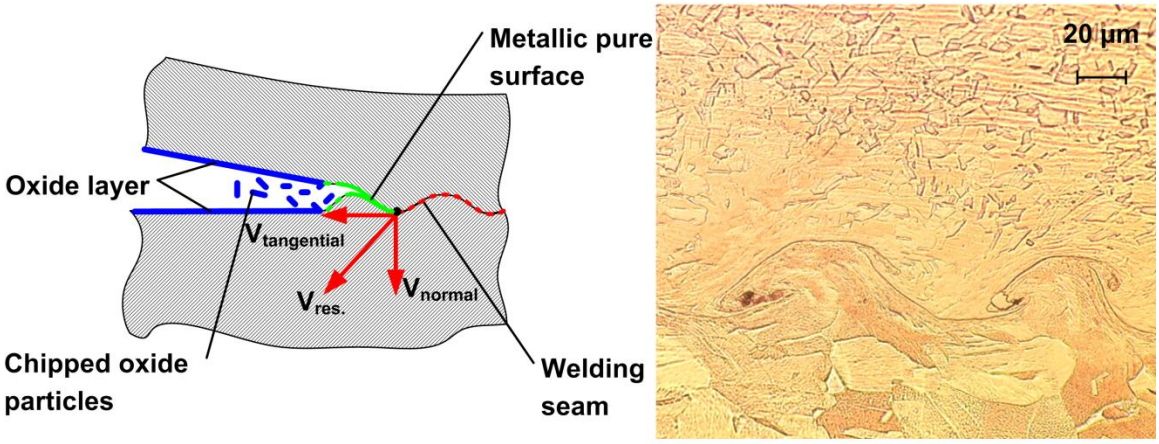

Figure 1: Schematic of oxide layer delamination and microsection of Cu-Cu EMPT weld.

For the electrical interconnection of Nb_3Sn/Cu composite wires two fundamental different concepts were tried: (1) direct joining of two wires by EMPT compaction with a Cu bushing as shown in Figure 2 with an overlap length of 1 cm, (2) the Nb_3Sn/Cu splices were placed on a Cu cone and a bushing was EMPT welded onto the cone with an overlap length of around 2 cm (Figure 3). The Nb_3Sn strands are joined before reaction.

Figure 2: Photograph and cross-section of Nb_3Sn strands connected to a Cu-bush with EMPT.

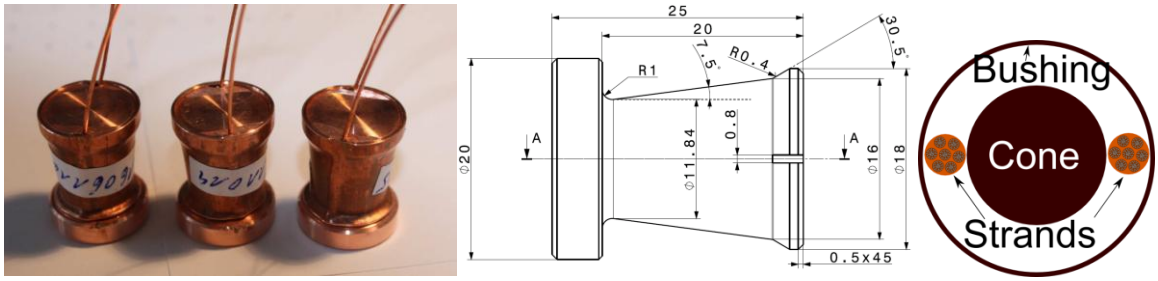

Figure 3: Nb_3Sn/Cu splices produced with an intermediate Cu cone. Preparation of soldered splice samples

2.3 Preparation of splices by soft soldering

Nb_3Sn strands have been reacted in glass tubes to keep them straight. The reacted strands were soldered onto 1-5 cm long Cu plates, either with Sn96Ag4 or with Sn77.2In20Ag2.8 solder alloys, using a soldering gun. Round Sn96Ag4 solder containing fluxing agent and a strip of Sn77.2In20Ag2.8 have been used. If needed additional fluxing agent was used to obtain good solder wetting and spreading.

2.4 Resistance measurements

The electrical resistance of splices immersed in liquid Helium at 4.2 K has been measured at the University of Karlsruhe with the four-points probe method in self-field. The resistance of the EMPT samples has been measured with test currents of 400 A, 600 A, 800 A and 1000 A. The resistance of the soldered splices was measured with a test current of 1000 A only. The voltage across the splices was measured with a Keithley Model 2182a nanovoltmeter. The voltage taps were placed at the edges of each splice. Two different assemblies have been prepared for soldered and EMPT splices (see Figure 4). The plates are electrically connected in series. For each solder alloy a total of five splices were tested, with an overlap length of 1, 2, 3, 4 and 5 cm. The Nb_3Sn strands were soldered onto Cu plates to be able to power them in series. To minimize heating of the Cu plates additional superconducting strand was added onto the plates.

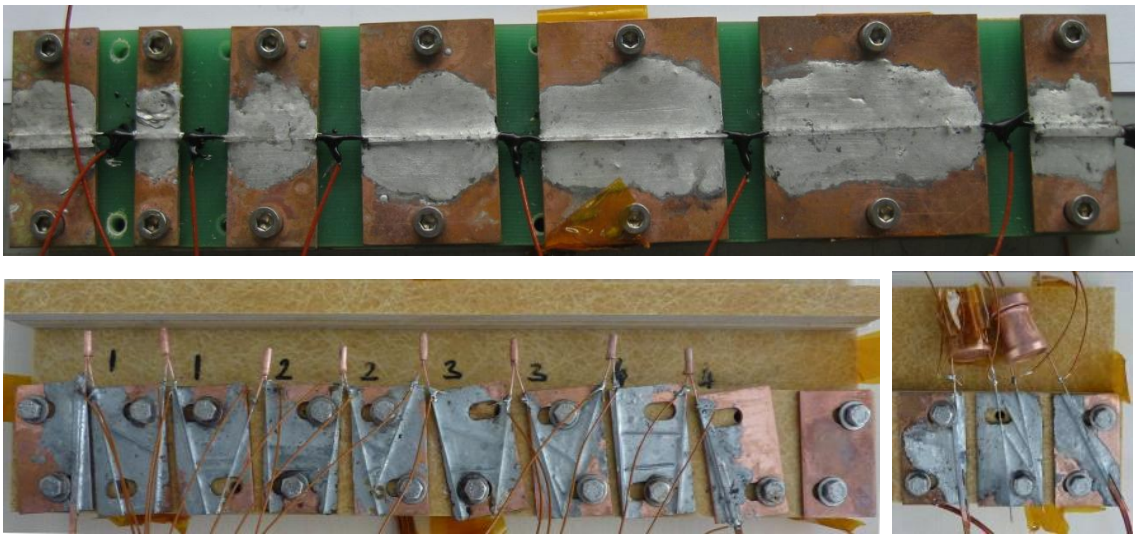

Figure 4: Set-up for 4.2 K resistance measurements of solder and EMPT Nb_3Sn lap joints.

2.5 Metallographic examination

After 4.2 K resistance measurements, all samples were characterized by optical metallography, and indentation hardness measurements. The splices have been cut in the center to determine the distance between the Nb_3Sn/Cu strands and filaments as input for the numerical model. Vickers hardness measurements in metallographic cross sections have been performed in order to estimate the RRR of the OFE Cu parts of the splices [8]. In addition peel tests on non reacted EMPT splices have been performed in order to verify if welding had been achieved during the EMPT process.

3 Results

3.1 Solder alloy electrical resistivity

The resistivity of the different solder alloys at cryogenic temperatures has been determined at CERN [3]. Figure 5 summarizes the electrical resistivity values for different solder alloys as a function of temperature.

In order to investigate the influence of the resistivity of the solder on the overall splice resistance, for the present study two solder materials with strongly different electrical resistivity at cryogenic temperatures have been selected, notably Sn96Ag4 and Sn77.2In20Ag2.8. The corresponding resistivity values at 4.2 K are 0.42 nΩ m and 67 nΩ m.

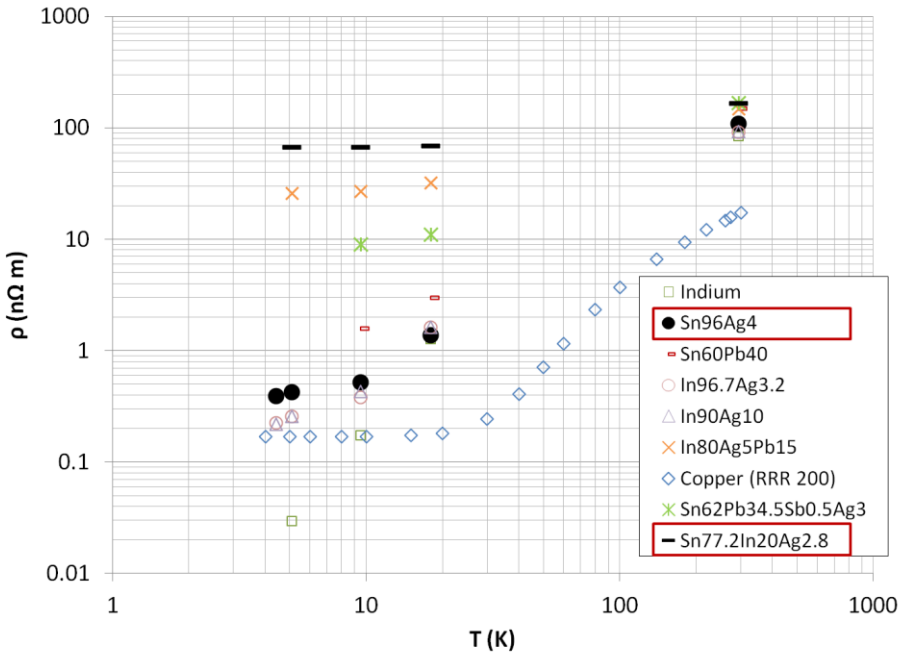

Figure 5: Electrical resistivity ρ as a function of the temperature T of selected solder alloys. The solders selected for this study are Sn96Ag4 and Sn77.2In20Ag2.8. For comparison the resistivity of Cu with an RRR of 200 is also shown.

3.2 Electrical resistance of splices produced by soft soldering

The resistance results of the lap joints with different overlap lengths produced with Sn96Ag4 and Sn77.2In20Ag2.8 solder alloys are summarized in Figure 6. For the soldered splices resistance measurements have been measured only with a test current of 1000 A, which corresponds approximately to the operating current of the prototype wiggler magnet. As expected, the splice resistance is roughly inversely proportional to the splice contact length, in the plot a $1/l$ fit is considered for each set of data.

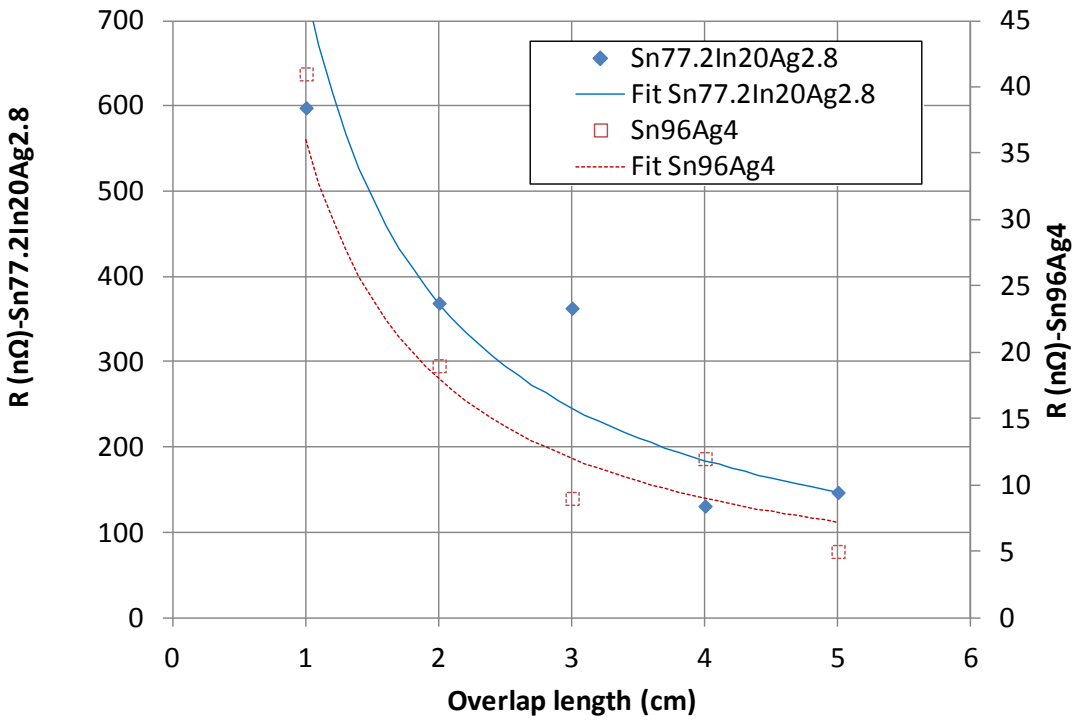

Figure 6: Electrical resistance (R) at 1000 A for lap joints immersed in liquid He with different overlap lengths produced with Sn96Ag4 and Sn77.2In20Ag2.8 solder alloys.

In average the splices produced with Sn77.2In20Ag2.8 and Sn96Ag4 solder alloys have a resistance of 740±220 nΩ and 36±10 nΩ (1 σ error) per 1 cm overlap length. Thus, the Sn77.2In20Ag2.8 soldered splice resistance is about 20 times higher than the resistance of the Sn96Ag4 soldered splices. This shows that the high resistivity of the Sn77.2In20Ag2.8 solder has a dominating influence on the overall splice resistance. The scatter of the normalized resistance results may partly come from different distances between the two soldered strands, or by solder imperfections.

3.3 Electrical resistance of splices produced by EMPT

The electrical resistance results for EMPT splices that have been produced with different process parameters are presented in Figure 7 as a function of the test current. There is a systematic trend of a resistance increase with increasing current, presumably due to splice heating with increasing current.

Samples 3a, 3b, 4a, 4b are lap joints with 1 cm overlap, and samples 5a and 5b are splices produced with an intermediate Cu cone and an overlap of about 2 cm.

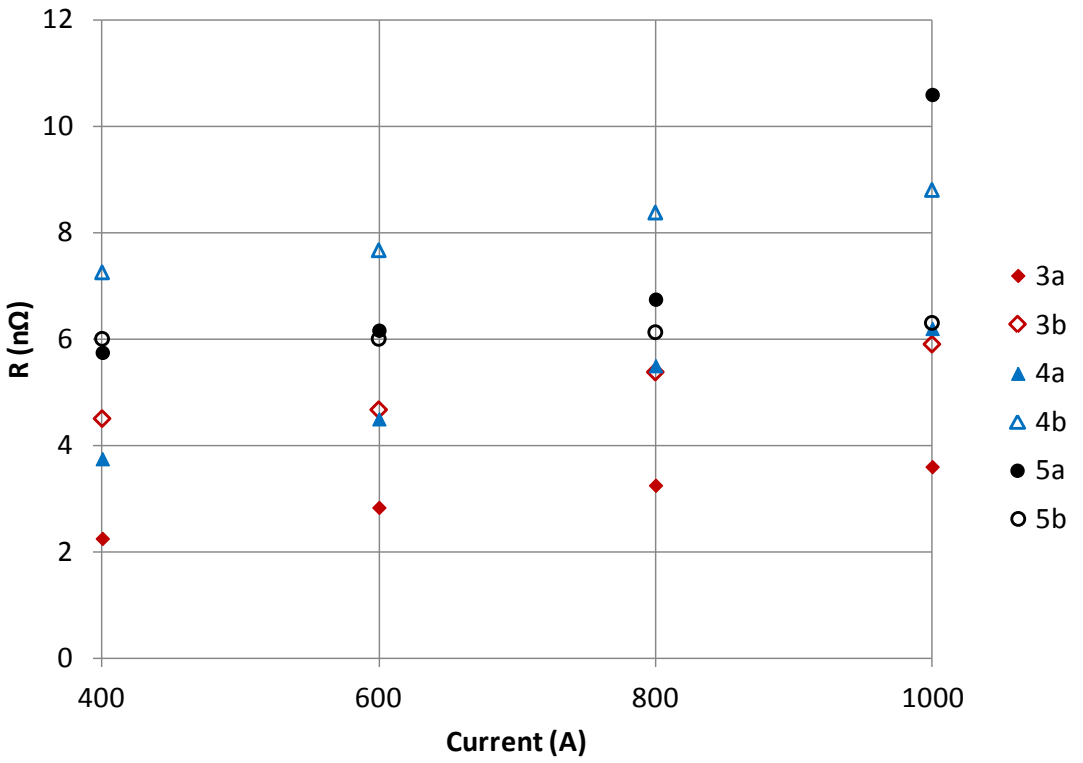

Figure 7: Electrical resistance (R) of EMPT splices immersed in liquid He as a function of the test current.

The resistance values measured with a test current of 1000 A, which is approximately the operating current, are summarised in Table 1. The results indicate that low resistances can be achieved with lap joints as well as with the splices produced with Cu cones.

Table 1: Electrical resistance for different splices produced by EMPT measured with a current of 1000 A.

Sample	Technique	Overlap length (cm)	R (nΩ)
3a	Lap joints	1	3.6
3b		1	5.9
4a	Lap joints	1	6.2
4b		1	8.8
5a	Intermediate Cu cones	2	11
5b		2	6.3

3.4 Estimation of the copper RRR from indentation hardness measurements

The indentation hardness of different splice components was measured with a Leica VMHT MOT hardness tester using a Vickers diamond pyramid indenter in the metallographic strand cross sections. A test load of 2 kg was applied during 15 s, and an objective with a magnification factor of 10 has been used. The RRR measurements have been performed with the set-up described in [9].

For the estimation of the Cu RRR from the Vickers hardness (HV2.0) values a series of RRR and HV2.0 measurements has been performed for high purity Cu samples with different degree of cold work. The following linear correlation between Vickers hardness (HV) and the RRR has been found (see Figure 8):

$$RRR = a \times HV2.0 + b, \tag{1}$$

with a=-3.976 and b=482.

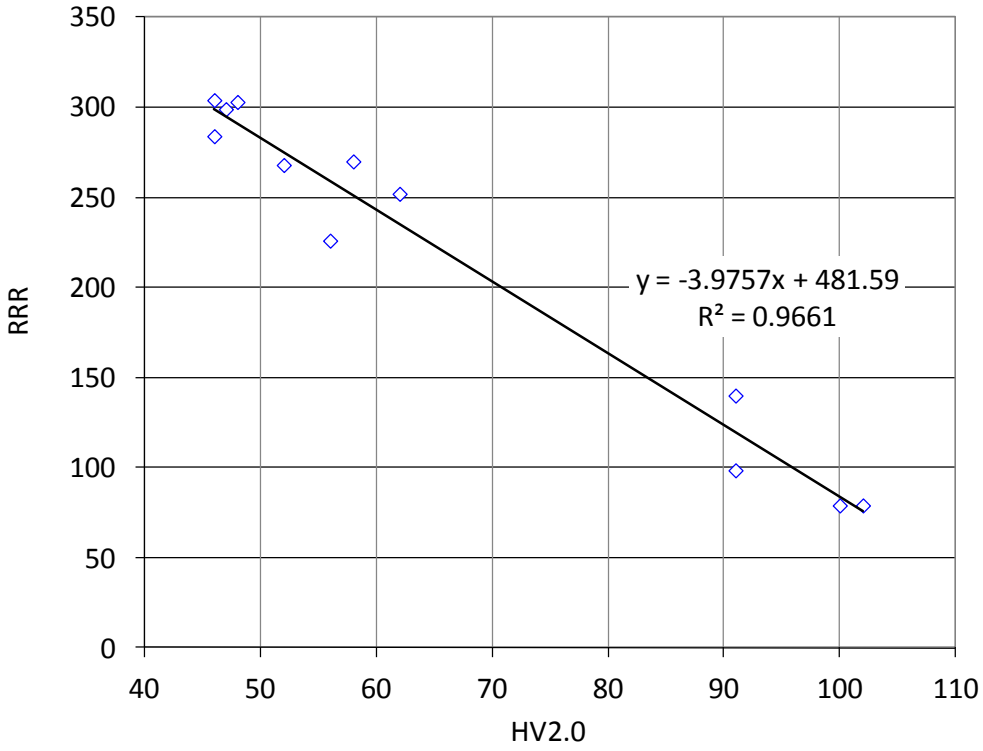

Figure 8: RRR as a function of Vickers hardness (HV2.0) for high purity OFE Cu with different degree of cold work [8].

3.5 Splice resistance simulations

FE simulations with Comsol Multiphysics were performed in order to investigate the influence of the splice dimensions and electrical material properties on the overall electrical splice resistance.

3.5.1 Soldered splices

In all solder splices the distance between the strands has been measured in the optical micrographs taken in the splice center (see Figure 9). The average distances between the two strands of the soldered lap joints are 104 µm and 87 µm for the Sn96Ag4 and Sn77.2In20Ag2.0 soldered splices, respectively.

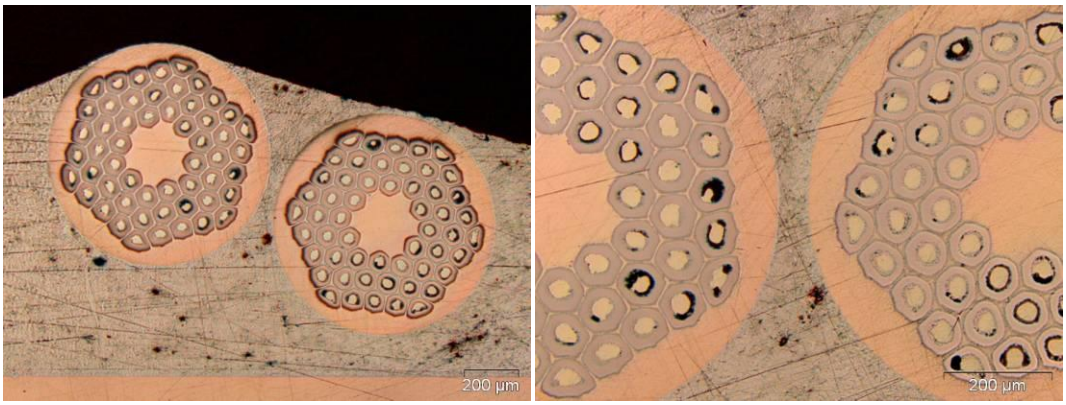

Figure 9: Metallographic cross section of a splice soldered with Sn77.2In20Ag2.8 solder alloy with 4 cm strand overlap length.

For the simulations only the bulk resistivities of the Cu parts and the solder have been considered. The additional resistance possibly caused by thin intermetallic layers, constriction resistances due to porosity and contact resistances are not taken into account [10,11]. The resistance of the thin unreacted diffusion Nb-Ta barriers in the RRP strand is neglected as well.

The electrical resistivity values of 67 nΩ m and of 0.42 nΩ m for the Sn77.2In20Ag2.8 and for the Sn96Ag4 solder alloys are taken from Figure 5. From HV2.0 measurements the RRR of the 50 mm wide Cu-plate and of the stabilising Cu in the superconducting strands is estimated to be 100 and 300 (see Equation 1). Simulations show that the RRR of the Cu-plate has a negligible influence on the splice resistance. All calculations were performed for a strand overlap length of 1 cm.

Figure 10 compares the calculated resistance for splices soldered with Sn77.2In20Ag2.8 and Sn96Ag4 solder alloys as a function of the distance between the Nb_3Sn/Cu strands.

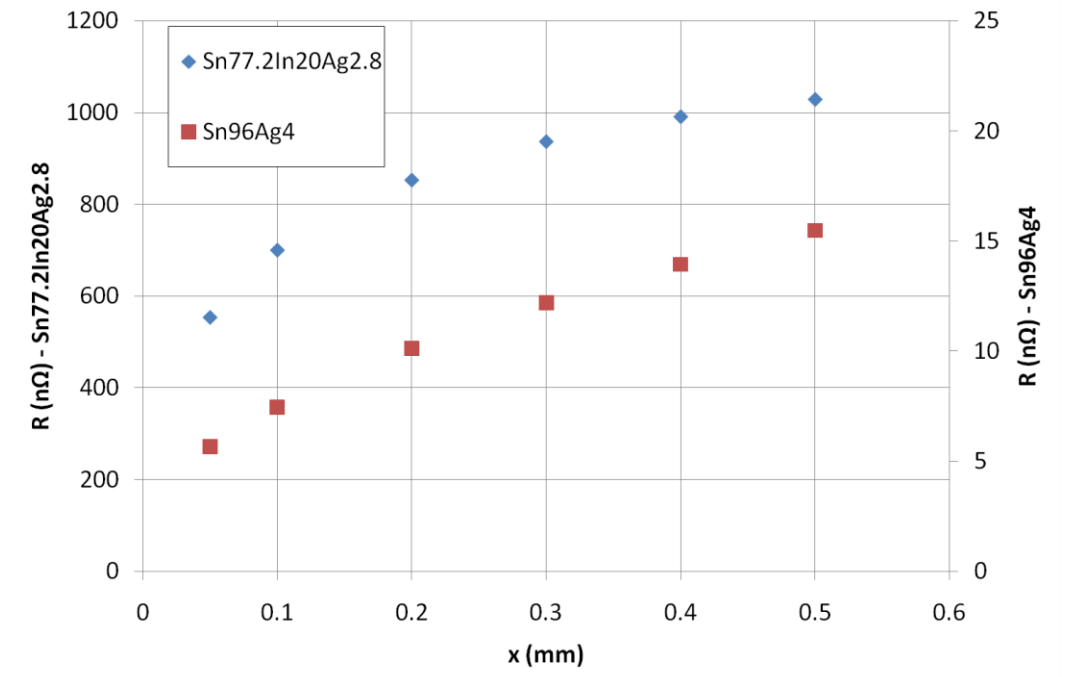

Figure 10: Simulated splice resistance R as a function of the distance between the opposing strands (x) for splices joined with different solder alloys. The splice overlap length is 1 cm.

In Table 2 the calculated and measured resistance results are compared, assuming a distance between the strands of 0.1 mm, which is the approximate average distance determined in the metallographic cross sections of the soldered splices. The calculated splice resistance produced with the high resistivity Sn77.2In20Ag2.8 solder alloy is in good agreement with the measured resistance. However, for the splices produced with the low resistivity solder Sn96Ag4 the calculated resistance is about 5 times lower than the measured resistance, indicating that in this case the splice resistance is not dominated by the solder alloy bulk resistance.

Table 2: Comparison between the measured and the simulated 4.2 K electrical resistance for lap joints produced by soft soldering with Sn77.2In20Ag2.8 and Sn96Ag4 (distance between the strands=0.1 mm, overlap length=1 cm).

	Sn77.2In20Ag2.8	Sn96Ag4
Experiment	740±220 nΩ	36±10 nΩ
Calculated	701 nΩ	7.5 nΩ

3.5.2 Splices produced by EMPT with Cu-bush

For the simulations only the bulk resistance of the Cu parts has been considered. A RRR of 325 is estimated for the stabilising Cu from the Vickers hardness $HV_{2.0}$=39±0.5 (1 σ error) that has been measured in the metallographic cross sections. The splice dimensions were taken from the metallographic cross section shown in Figure 11.

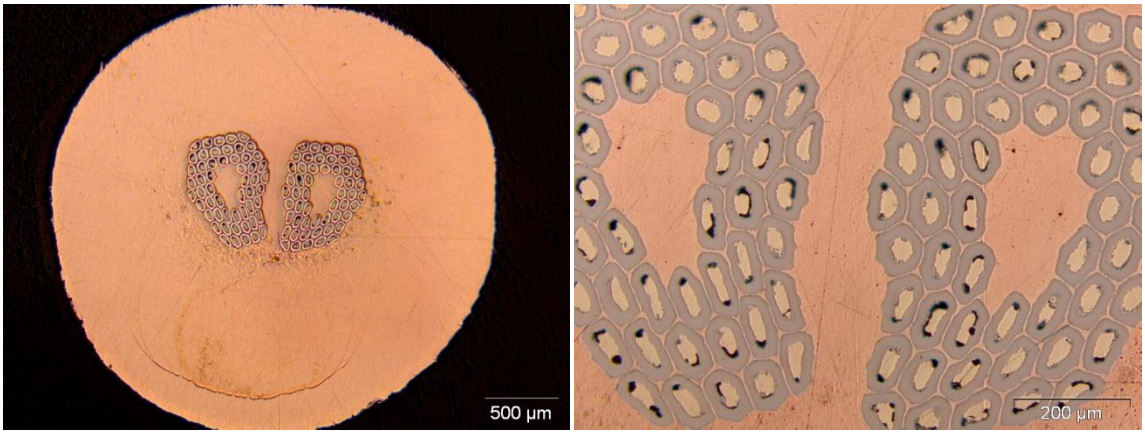

Figure 11: Metallographic cross section of EMPT splice sample 3b produced with Cu bush.

The resistance for a perfectly welded splice with 1 cm overlap is 0.7 nΩ, assuming a RRR of the stabilising Cu of 325, which is the value estimated from indentation hardness measurements in the external wire part. For comparison, the lowest measured resistance measured for an EMPT splice with Cu bushes is 3.6 nΩ (see Table 1).

The potential influence of a strongly varying RRR of the interfilament Cu, which could possibly come from Sn contamination during the superconductor reaction [12], on the

overall splice resistance has been calculated. Figure 12 compares the current flow for two different RRR values of the Cu between the filaments. When the RRR of the interfilament Cu is drastically decreased from 300 to 1, the overall splice resistance is only increased from 0.75 nΩ to about 1.9 nΩ. Thus, provided that welding between the strands can be achieved, very low splice resistances are obtained even when the interfilament Cu would exhibits an extremely poor RRR. It is therefore concluded that the splices produced with Cu bushes are not perfectly welded, which is also confirmed by peel tests after removing the bushes.

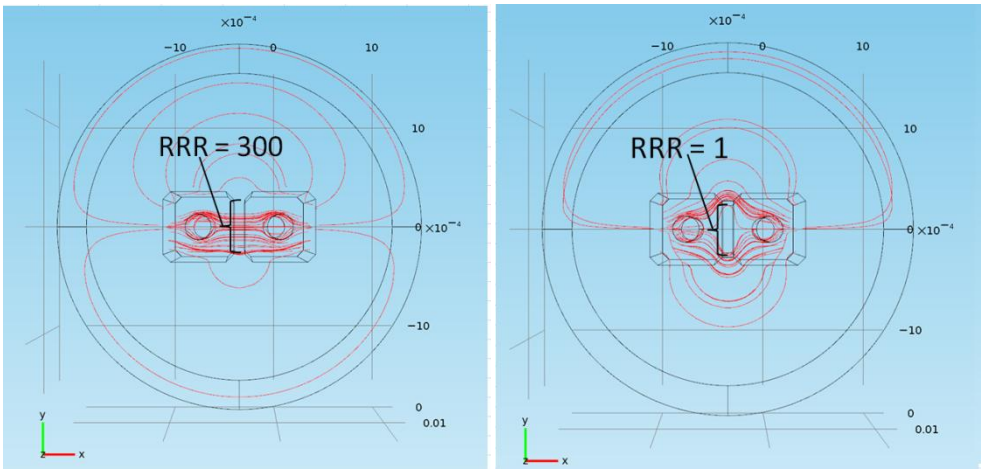

Figure 12: Streamlines of the current density for different RRR values of the Cu between the filaments. Left and right image correspond to an interfilament Cu RRR of 300 and 1, respectively. The RRR of the external Cu is 300 and the distance between the filaments is 0.1 mm.

3.5.3 Splices produced by EMPT with an intermediate Cu-cone

Metallographic cross sections of the connection of the two strands to a Cu cone are shown in Figure 13. In the FE model the splice geometry has been simplified and chamfer and radii smaller than 1 mm have been neglected. An RRR of 330 is estimated for the Cu cones from the indentation hardness measured in the metallographic cross section ($HV_{2.0}$=38±1, 1 σ error).

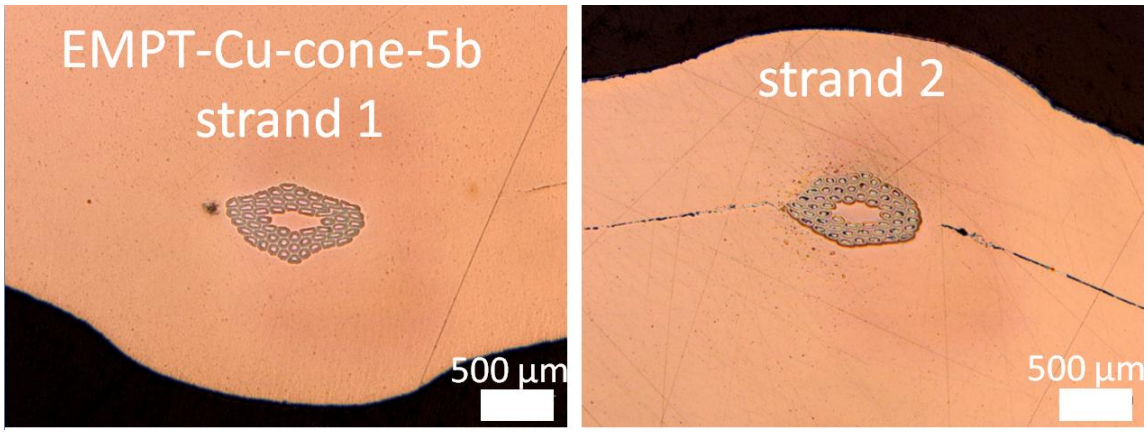

Figure 13: Metallographic cross sections of sample EMPT-Cu-cone-5b.

The 4.2 K splice resistance is nearly inversely proportional to the RRR of the Cu cone. The resistance of 7.5 nΩ that is calculated assuming a RRR of 330 is in good agreement with the experimental resistance values (6.3 nΩ and 11 nΩ), indicating that the splice resistance is determined by the Cu bulk resistance, and that welding between the different Cu parts has been achieved by the EMPT process. This is also confirmed by peel tests, which show that the strands have been indeed welded to the Cu cones.

The simulations also show that when the superconducting strands are connected to the Cu-cone adjacent to each other with a distance of about 1.5 mm (see Figure 14), the overall 4.2 K splice resistance decreases from 7.5 nΩ to 4.4 nΩ (with an overlap length of 2 cm). The splice resistance can be further decreased when the contact length between strands and Cu cone is increased.

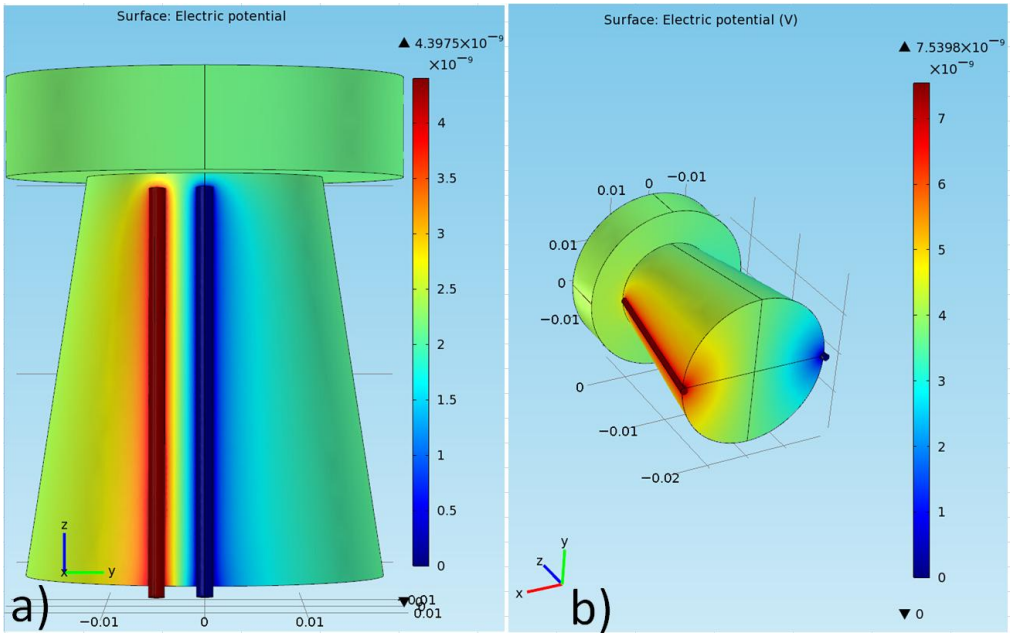

Figure 14: FE model showing the potential distribution on the surfaces of the EMPT splices with Cu cones. (a) with adjacent and (b) with opposing strands.

4 Discussion

Soft soldering is the most commonly used method for the electrical interconnection of superconducting strands and cables. The electrical resistance of soldered joints is influenced by the bulk resistance of the non-superconducting joint components (Cu stabiliser, diffusion barriers and solder alloy), constrictions of the current flow, the resistance of intermetallic layers and possibly contact resistances at the joint interfaces. Here we have studied the influence of the solder alloy resistivity on the overall resistance of soldered Nb_3Sn/Cu lap joints. For this purpose we have selected solder alloys with strongly differing bulk resistivity (the 4.2 K resistivity of Sn77.2In20Ag2.8 is about 160 times higher than that of the Sn96Ag4 solder).

The fact that the 4.2 K resistance of splices produced by soft soldering with Sn77.2In20Ag2.8 is about 20 times higher than the resistance of splices with the same

geometry produced with Sn96Ag4 shows that the solder resistivity can have a strong influence on the splice resistance. Indeed, a comparison between experimental results and calculated splice resistances confirms that when using a high resistivity solder like Sn77.2In20Ag2.8 the joint resistance is determined by the resistance of the solder layer.

However, when taking into account only the bulk resistance of the stabilizing Cu and a 0.1 mm-thick pure Sn96Ag4 solder layer, the calculated joint resistance is almost 5 times lower than the measured resistance. This may indicate that the RRR of the pure Sn96Ag4 solder is reduced by diffusion of contaminating elements during the soldering process, and/or that in splices with low solder layer resistances the contribution of other resistances (intermetallic layer resistances, constriction resistance and contact resistances at the joint interfaces) is dominating the overall resistance.

Soft soldering of Nb_3Sn/Cu splices is only possible with the brittle conductor, with the associated risk of conductor damage. Therefore, we are studying methods that can be applied to the ductile Nb_3Sn precursor wires before the reaction. Here we present EMPT as a new method for manufacturing Nb_3Sn lap joints. With this method splice resistances well below 10 nΩ can be achieved.

The resistance of the EMPT splices with Cu cones can be predicted when assuming that the splice resistance is only determined by the resistance of the Cu between the superconducting filaments, which shows that the wires are indeed welded onto the cones. Welding of strands onto the Cu cones is also confirmed by peel tests. The comparison between simulations and experimental results for the EMPT welded splice with Cu cones also confirms that the thin Nb-Ta diffusion barriers in the RRP strands do not strongly influence the splice resistance [4]. The 4.2 K electrical resistance of EMPT splices with Cu cones can be further reduced by placing the two superconducting strands adjacent to each other, and or by increasing the overlap length.

In contrast to the splices with Cu cones, the measured resistance of lap joints produced by EMPT is higher than the simulated resistance, suggesting that the wires are not perfectly welded to each other, which is confirmed by wire peel tests after removing the bushes.

EMPT welding implies plastic deformation of the strands, which may somewhat degrade the superconductor performance. A slight strand degradation should be acceptable when splices can be placed in low-field areas. Also it is reported in [13] that the OST RRP strand can be deformed by around 30% without any major negative impact on the critical current.

The splices produced by EMPT are mechanically and thermally stabilized because additional high purity Cu bushes are welded around the strands. In addition, massive Cu cones can further increase the heat capacity of the splices, and they can be used as mechanical support as well.

Another solid state welding method that can produce metallic bonds between the matrix of Nb_3Sn/Cu strands without Cu melting and without intermediate filler material is US welding, which may therefore be another promising technique for the electrical interconnection of ductile Nb_3Sn/Cu precursor strands.

5 Conclusion

EMPT can be considered for the electrical interconnection when a large number of Nb_3Sn/Cu splices needs to be produced, for instance for horizontal racetrack damping wiggler magnets as they are studied for CLIC. Ductile Nb_3Sn/Cu pre-cursor strands can be connected and splice resistance values below 10 nΩ at 4.2 K can be achieved with 1 cm overlap length. Massive high purity Cu cones can be added to the splice for thermal and mechanical stabilisation. Manipulating the brittle strands after reaction is not required, which strongly reduces the risk of damaging the strands.

Generally soldered splices exhibit a higher resistance than splices produced by solid state welding with the same overlap length. The resistance of soldered splices is strongly dependent on the solder bulk resistivity. When using a high resistivity solder like Sn77.2In20Ag, the splice resistance is mainly determined by the solder resistance. The splice resistance can be strongly reduced by a factor of 20 when using a low resistivity solder like Sn96Ag4 instead of a high resistivity solder.

Acknowledgements

The authors want to thank Andreas Grau, Karlsruhe Institute of Technology (KIT), for electrical resistance measurements, Axel Bernhard, KIT for enabling us to measure at CASPER. Bruno Meunier, CERN we want to thank for manufacturing the sample holders. Noel Dalexandro, CERN we want to thank for discussions on soldering techniques.

References

1 R. Tomas, "Overview of the CLIC Compact Linear Collider", PRST-A&B 13, 01480 (2010)

2 F. Heringhaus, T.A. Painter, "Magnetoresistance of selected Sn- and Pb-based solders at 4.2 K", Materials Letters, 57(4), (2002), 787

3 S. Heck, C. Scheuerlein, P. Fessia. S. Triquet, A. Bonasia, "*Resistivity of different solder alloys at cryogenic Temperatures*", CERN Internal note, EDMS Nr: 1133529, (2011)

4 C. Scheuerlein, D. Schoerling, S. Heck, IEEE Trans. Appl. Supercond., 21(3), (2011), 1791

5 J.P. Tock, D. Bozzini, F. Laurent, S. Russenschuck, B Skoczen. Electro-mechanical aspects of the interconnection of the lhc superconducting corrector magnets. CERN-LHC-Project-Report-724, 2004.

6 J. A. Parrell, Y. Zhang, M. B. Field, P. Cisek, and S. Hong, IEEE Trans. Appl. Supercond. 13(2), (2003), 3470.

7 R. Schäfer, P. Pasquale: "Industrial Application of the Electromagnetic Pulse Technology", http://www.english.pstproducts.com/downloads.htm

8 S. Heck., C. Scheuerlein. P. Fessia. R. Principe, "*The RRR of the Cu components of the LHC main busbar splices*", technical note EDMS 1057918, 2010 CERN.

9 Z. Charifouline, IEEE Appl. Supercond. 16(2), (2006), 1188

10 C. Scheuerlein, M. Taborelli, M. Cantoni, Appl. Surf. Sci, 253 (3), (2006), 1393

11 C. Scheuerlein, Ph. Gasser, P. Jacob, D. Leroy, L. Oberli, M. Taborelli, J. Appl. Phys. 97(3), (2005)

12 F. R. Fickett, Cryogenics 22, (1982), 135

13 A.A. Polyanskii, P.J. Lee, M.C. Jewell, E. Barzi, D. Turrioni, A.V. Zlobin, D.C. Larbalestier, Supercond. Sci. Technol., 22, (2009), 1–13